Matter and Radiation at Extremes | RESEARCH ARTICLE | scitation.org/journal/mre

High pressure effects on the excitation spectra and dipole properties of Li, Be^{+}, and B^{2+} atoms under confinement

Cite as: Matter Radiat. Extremes 5, 024401 (2020); doi: 10.1063/1.5139099
Submitted: 20 November 2019 • Accepted: 16 January 2020 •
Published Online: 9 March 2020

C. Martínez-Flores[1] and R. Cabrera-Trujillo[2,3,a)]

AFFILIATIONS

[1] Departamento de Química, Universidad Autónoma Metropolitana Iztapalapa, San Rafael Atlixco 186, Col. Vicentina, Iztapalapa, C.P. 09340 México D.F., Mexico
[2] Instituto de Ciencias Físicas, Universidad Nacional Autónoma de México, Ap. Postal 43-8, Cuernavaca, Morelos, 62251, Mexico
[3] Theoretische Chemie, Physikalisch-Chemisches Institut, Universität Heidelberg, INF 229, 69120 Heidelberg, Germany

[a)] **Author to whom correspondence should be addressed:** trujillo@icf.unam.mx

ABSTRACT

Properties of atoms and molecules undergo significant changes when subjected to spatial confinement. We study the excitation spectra of lithium-like atoms in the initial $1s^2 2s$ electronic configuration when confined by an impenetrable spherical cavity. We implement Slater's X-α method in Hartree–Fock theory to obtain the excitation spectrum. We verify that as the cavity size decreases, the total, 2*s*, 2*p*, and higher excited energy levels increase. Furthermore, we confirm the existence of crossing points between *ns*–*np* states for low values of the confinement radius such that the $ns \rightarrow np$ dipole transition becomes zero at that critical pressure. The crossing points of the *s*–*p* states imply that instead of photon absorption, one observes photon emission for cavities with radius smaller than the critical radius. Hence, the dipole oscillator strength associated with the $2s \rightarrow 2p$ transition becomes negative, and for higher pressures, the $2s \rightarrow 3p$ dipole oscillator strength transition becomes larger than unity. We validate the completeness of the spectrum by calculating the Thomas–Reiche–Kuhn sum rule, as well as the static dipole polarizability and mean excitation energy of lithium-like atoms. We find that the static dipole polarizability decreases and exhibits a sudden change at the critical pressure for the absorption-to-emission transition. The mean excitation energy increases as the pressure rises. However, as a consequence of the critical transition from absorption to emission, the mean excitation energy becomes undetermined for higher pressures, with implications for material damage under extreme conditions. For unconfined systems, our results show good to excellent agreement with data found in the literature.

I. INTRODUCTION

Confined quantum systems exhibit significant changes to their structure, stability, reactivity, binding interactions, dynamics, and spectra as a consequence of modifications to the spatial boundary conditions in the presence of an extreme environment. Atoms or molecules within cavities, organic/inorganic host–guest complexes, quantum dots, fullerenes, and nanotubes are examples of real quantum confined systems. The main objective when studying confined quantum systems is to construct an accurate theoretical model that takes into account changes in the electronic wave-function and energy levels due to the boundary conditions imposed by the surrounding environment. In this respect, theoretical calculations can be realized by adopting a suitable choice of boundary conditions. The pioneering work of Michels *et al.*[1] provided the first model of a hydrogen atom confined in an impenetrable spherical cavity to simulate the effect of pressure. In recent years, the topic of confined atoms has attracted much attention and has become a very active field of research.[2–5] Reviews with detailed discussion of the progress in this field can be found in Refs. 2–6 and references therein.

To describe the electronic structure and interactions of a multi-electron system, a variety of theoretical methods have been developed, including, among others, Hartree–Fock (HF) theory and density functional theory (DFT), and these have had great success in different problems in atomic physics.[6–11] Owing to the complexity of the *N*-body problem, some approximations have been implemented, in addition to having the system under confinement by spatial limitation of the electrons, which leads to

complications in the one- and two-electron integrals. A widely used approach to the treatment of N-body systems is to consider a pseudopotential that describes the inner electronic structure of the atom. The basic idea of pseudopotentials is to take into account the multi-electron core interaction with a single valence electron by using a modified Coulomb potential.[7,8,11] Such pseudopotential approaches have been used to describe the electronic spectra of confined systems.[12,13] Lin and Ho[12] used a pseudopotential for the lithium atom to simulate the core interaction with the single valence electron with optimized parameters. They calculated the photoionization cross section of the 2s shell electron under confinement by a power exponential potential due to an endohedral cavity and found that multiple Cooper resonances emerged.[14] Their results show the importance of cage thickness and a smooth shell boundary in the photoionization cross section. Another example is due to Sarsa *et al.*,[13] who studied the effects of confinement on the outer valence electrons for the ground state configurations of carbon and iron atoms. In standard HF theory, the main complication that arises when dealing with quantum confined systems is the treatment of the one- and two-electron integrals, particularly the electron exchange integral, as shown by Ludeña.[15] Fortunately, Slater[16] proposed a simplified approach to treat the electron exchange operator in the HF method by replacing it by a term proportional to the charge density of the inner electrons. This approach has been fruitful in treating problems in atomic and molecular structure with satisfactory results,[17] particularly in the development of DFT theory. However, to the authors' knowledge, there have not been any studies of the effects of confinement on the excitation spectra of a multi-electron system in the context of HF theory by means of Slater's X-α approach.

The goal of this work is to apply Slater's X-α approach to the ground and excited states of Li-like atoms confined in an impenetrable spherical cavity. To show the strength of Slater's X-α approach to the calculation of the excitation spectrum of atoms, we take as a benchmark example the ground states of lithium-like atoms in the initial electronic configuration $1s^2 2s$, adopting a restricted HF approach. We focus on the dipole oscillator strength (DOS) and derived properties such as the static dipole polarizability and the mean excitation energy.

The remainder of this paper is organized as follows. In Sec. II, we present the theoretical approach used to study the influence of a spherical confinement cavity on lithium-like atoms. In Sec. III, we discuss our results and findings. In Sec. IV, we give our conclusions and perspectives. Note that we use atomic units (a.u.) throughout, unless physical units are explicitly stated.

II. THEORY

A. Slater's X-α approach in Hartree–Fock theory

In this section, we present the HF method to obtain the $1s^2 2s$ ground state energies of Li, Be^+, and B^{2+} atoms, incorporating confinement conditions.

In an HF approach, the total wavefunction is defined as a Slater determinant $\Psi(r) = N \det\{\psi_i\}$, where N is a normalization constant. The general restricted HF approach[18] considers the two electrons in the $1s^2$ core to be in the same orbital. To simplify the calculation of the excitation spectra, we assume that the inner electrons do not see the outer electrons. This approach is known as the frozen-core approximation, which is usually treated within a pseudopotential approach.[7,8,11] However, here we do not use any specific pseudopotential formula to describe the interaction of the inner electrons, since this is calculated explicitly for every confinement configuration in a self-consistent manner. Then, for the ground state of a lithium-like atom, the HF equations are

$$(\hat{h}_1 + \hat{J}_1)\psi_1(\mathbf{r}) = \epsilon_1 \psi_1(\mathbf{r}), \tag{1}$$

$$(\hat{h}_2 + 2\hat{J}_1 - \hat{K}_1)\psi_2(\mathbf{r}) = \epsilon_2 \psi_2(\mathbf{r}), \tag{2}$$

where ϵ_j are the eigenvalues, ψ_j are the eigenfunctions, h_j are the one-electron operators, and $\hat{J}_j$ and $\hat{K}_j$ are the two-electron Coulomb and exchange operators, respectively. These operators are defined as

$$\hat{h}_j(\mathbf{r}) = -\frac{1}{2}\nabla_j^2 - \frac{Z}{r} + V_c(r), \tag{3}$$

$$\hat{J}_j(\mathbf{r})\psi_i(\mathbf{r}) = \left[\int dr_2 \, \frac{\psi_j^*(\mathbf{r}_2)\psi_j(\mathbf{r}_2)}{r_{12}}\right]\psi_i(\mathbf{r}), \tag{4}$$

$$\hat{K}_j(\mathbf{r})\psi_i(\mathbf{r}) = \left[\int dr_2 \, \frac{\psi_j^*(\mathbf{r}_2)\psi_i(\mathbf{r}_2)}{r_{12}}\right]\psi_j(\mathbf{r}), \tag{5}$$

where $r_{12} = |\mathbf{r} - \mathbf{r}_2|$. The one-electron operator, Eq. (3), includes the confinement potential $V_c(r)$ (see below). The total ground state energy of the confined system is given by

$$E_{\mathrm{HF}} = 2\hat{h}_{11} + \hat{h}_{22} + \hat{J}_{11} + 2\hat{J}_{12} - \hat{K}_{12}. \tag{6}$$

It can be seen that Eq. (1) is in eigenvalue form, so the excitation spectra of the core electron can be readily obtained. However, Eq. (2) is not, owing to the presence of the exchange operator, Eq. (5). To have an eigenvalue equation, we resort to Slater's X-α approach,[16] in which the exchange operator is replaced by

$$\hat{K}_1(\mathbf{r})\psi_2(\mathbf{r}) = \alpha_X \rho_1^{1/3}(\mathbf{r})\psi_2(\mathbf{r}), \tag{7}$$

where α_X is a parameter, and $\rho(\mathbf{r})$ is the charge density due to the $1s^2$ inner electrons[18] and is given by

$$\rho_1(\mathbf{r}) = 2|\psi_1(\mathbf{r})|^2, \tag{8}$$

with $\psi_1(\mathbf{r})$ the eigenfunction of the core electrons. To solve the HF equations (1) and (2), we implement a finite-difference numerical approach within a self-consistent field (SCF) procedure to obtain the eigenvalues, eigenfunctions, and dipole-dependent properties. For each iteration, we calculate Eq. (5) explicitly and determine Slater's X-α constant as[19,20]

$$\alpha_X = \frac{\langle \psi_2(\mathbf{r})|\hat{K}_1(\mathbf{r})|\psi_2(\mathbf{r})\rangle}{\langle \psi_2(\mathbf{r})|\rho_1^{1/3}(\mathbf{r})|\psi_2(\mathbf{r})\rangle}, \tag{9}$$

finding the excitation spectrum of the 2s electron. The procedure is repeated until Eq. (6) has reached self-consistency within a 10^{-6} error difference for the total ground state energy.

Owing to the spherical symmetry of the system, we assume $\psi(\mathbf{r}) = R_l(r)Y_l^m(\theta,\varphi)$ and $R_l(r) = u_l(r)/r$, where Y_l^m are spherical harmonics. This is done for both core and valence wavefunctions.

We consider the lithium-like atoms to be confined by an impenetrable spherical cavity, so the confinement potential is given by[1–6]

$$V_c(r) = \begin{cases} 0, & r < R_0, \\ \infty, & r \geq R_0. \end{cases} \tag{10}$$

where R_0 is the confinement radius of the cavity and is commensurate with the confinement pressure (see below).

1. Finite-difference approach

As the finite-difference approach has been reported previously by Cabrera-Trujillo and Cruz,[21] here we just summarize our implementation to find the eigenvalues and eigenfunctions of Eqs. (1) and (2). The finite-difference approach consists in discretizing the function $u(r) \to u_k$ and $r \to r_k$, known at the kth point on a numerical grid, with $k = 0$ corresponding to u_0 and $k = N + 1$ to u_{N+1}, which are the boundary conditions of the system.[22] In our case, for the impenetrable cavity, $u_{N+1} = 0$ and $r_{N+1} = R_0$. We implement the finite-difference approach centered at the midpoint. With this, Eqs. (1) and (2) are rewritten as

$$\mathbf{H}\vec{\phi} = E\vec{\phi}, \tag{11}$$

where $\mathbf{H}$ is a tridiagonal symmetric matrix with N eigenvalues and eigenfunctions, and $\vec{\phi}$ is related to $\vec{u}$ by a linear transformation.[21]

We solve Eq. (11) in a grid box that extends from $r = 0$ to $r = R_0$, with a total of $N = 2000$ points spaced logarithmically in this range as a function of the confinement radius R_0. This logarithmic grid allows us to give a better description of the wavefunction cusp at the origin and a good number of continuum states. We have found that $N = 2000$ satisfies the Thomas–Reiche–Kuhn (TRK) sum rule up to five decimal digits. The accuracy of our finite-difference approach can be controlled by the number of points in the grid and their spacing; for example, for the free lithium atom, we obtain eigenvalues with precision up to the fifth decimal place. This approach gives a total of N excited states to describe the DOS electronic properties for each spherical cavity with radius R_0, per electron. The values of R_0 are chosen between 0.5 a.u. and 100 a.u. Our approach is implemented in a Fortran 95 code that calculates the eigenvalues, eigenfunctions, and physical properties of the system.

B. Physical properties

1. Dipole oscillator strengths

The DOS accounts for the transition probability from an initial state to a final excited state and is defined as

$$f_{n0} = 2\left(E^n_{\mathrm{HF}} - E^0_{\mathrm{HF}}\right)\left|\langle\Psi_n(\mathbf{r})|\sum_{i=1}^{N}\mathbf{r}_i\cdot\hat{\epsilon}\,|\Psi_0(\mathbf{r})\rangle\right|^2, \tag{12}$$

where $\hat{\epsilon}$ is the direction of momentum transfer or the polarization vector of the electromagnetic radiation. Here, E^0_{HF} and E^n_{HF} are respectively the initial and final total energies, with Ψ_0 and Ψ_n respectively the initial and final total wavefunctions for a given transition. Owing to the presence of just a single determinant and for an electron operator, as in the case of the dipole operator $\hat{O} = \Sigma_i \mathbf{r}_i$, the DOS are reduced to single-electron transitions from either the core or the valence electron.[18] Under the spherical symmetry of the system, Eq. (12) becomes[23,24]

$$f^i_{n0} = \frac{2}{3}\left(\epsilon^i_n - \epsilon^i_0\right)\left|\langle R^i_n(r)|r|R^i_0(r)\rangle\right|^2, \tag{13}$$

where the i stands for electron $i = 1$ (core electron transitions) or $i = 2$ (valence electron transitions). To confirm that our numerical approach has rendered a complete set of states, the TRK sum rule,[25] $\Sigma_n f_{n0} = N_e$, must be satisfied, i.e., $N_e = 3$. Note that for absorption, Eq. (13) is positive, but for emission, i.e., when $\epsilon^i_n < \epsilon^i_0$, the DOS becomes negative.

2. Static dipole polarizability

The static dipole polarizability is defined through the DOS [Eq. (12)], and is given by

$$\alpha_s = \sum_n \frac{f_{n0}}{\left(E^n_{\mathrm{HF}} - E^0_{\mathrm{HF}}\right)^2} = \sum_{i,n}\frac{f^i_{n0}}{\left(\epsilon^i_n - \epsilon^i_0\right)^2}, \tag{14}$$

where it exhibits an explicit dependence on the single-electron dipole oscillator strengths. Consequently, it can be rewritten as

$$\alpha_s = 2\alpha^{1s}_s + \alpha^{2s}_s, \tag{15}$$

where α^i_s is the contribution from the core ($i = 1$) or the valence ($i = 2$) electron. For photon absorption, the polarizability is positive, but for photon emission, it becomes negative.

3. Mean excitation energy

A parameter that characterizes the amount of energy loss when a swift heavy ion penetrates a target is provided by the mean excitation energy I_0, as defined by Bethe:[26]

$$\ln I_0 = \frac{\sum_n f_{n0}\ln\left(E^n_{\mathrm{HF}} - E^0_{\mathrm{HF}}\right)}{\sum_n f_{n0}} = \frac{\sum_{i,n} f^i_{n0}\ln\left(\epsilon^i_n - \epsilon^i_0\right)}{\sum_{i,n} f^i_{n0}}. \tag{16}$$

Using the TRK sum rule,[25] Eq. (16) can be rewritten as

$$\begin{aligned} 3\ln I_0 &= 2\sum_n f^{1s}_{n0}\ln\left(\epsilon^{1s}_n - \epsilon^{1s}_0\right) + \sum_n f^{2s}_{n0}\ln\left(\epsilon^{2s}_n - \epsilon^{2s}_0\right) \\ &= 2\ln I^{1s}_0 + \ln I^{2s}_0, \end{aligned} \tag{17}$$

which is the orbital decomposition or Bragg rule for the mean excitation energy, as used by Oddershede and Sabin[27] in energy loss deposition studies.

III. RESULTS

A. Unconfined lithium-like atoms

To show the reliability of our approach when applied to a multielectron system, we present in Table I the results for the unconfined Li, Be^+, and B^{2+} atoms. We show the core electron ground and excited orbital energies ϵ^{1s}_0 and ϵ^{2p}_0, the total HF energy E_{HF}, the DOS f^i_{is2p} for the first dipole transition, the polarizability α^i_s, and the mean excitation energy I^i_0. The same quantities are also reported for the valence ($2s$) electron. In the case of the ϵ^{1s}_0 and E_{HF} energy values for the Li, Be^+, and B^{2+} atoms, we observe good agreement up to four-decimal precision when compared with the results of Froese-Fischer.[28] For the Li atom mean excitation energy I^{1s}_0, we observe a difference of less than 5% with respect to the value reported by Oddershede and

TABLE I. Unconfined ground state properties for free Li, Be^+, and B^{2+} atoms. We report values for the core ($i=1$) and valence ($i=2$) electrons for the ground (ϵ_0^{is}) and excited (ϵ_0^{2p}) orbital energies, the total HF energy E_{HF}, the DOS f^i_{is2p}, the static dipole polarizability α^i_s, and the mean excitation energy I^i_0. Slater's α_X parameter, Eq. (9), takes the values $\alpha_X^{Li} = 0.580\,02$, $\alpha_X^{Be^+} = 0.526\,32$, and $\alpha_X^{B^{2+}} = 0.499\,22$.

	Core ($1s^2$)		
	Li	Be^+	B^{2+}
ϵ_0^{1s}	−2.792 32	−5.666 97	−9.541 58
	(−2.792 36)[a]	(−5.667 11)[a]	(−9.541 98)[a]
ϵ_0^{2p}	−0.508 09	−1.139 61	−2.021 42
E_{HF}	−7.236 33	−13.610 9	−21.985 4
	(−7.236 41)[a]	(−13.611 3)[a]	(−21.986 2)[a]
f^{1s}_{1s2p}	0.261 19	0.304 97	0.329 65
α^{1s}_s	0.102 45	0.027 49	0.010 24
I^{1s}_0	103.613	197.505	321.368
	(109.32)[b]	...	...
	Valence ($2s^1$)		
	Li	Be^+	B^{2+}
ϵ_0^{2s}	−0.201 16	−0.672 82	−1.397 22
	(−0.196 32)[a]	(−0.666 15)[a]	(−1.389 85)[a]
ϵ_0^{2p}	−0.138 61	−0.547 31	−1.210 49
E_{HF}	−7.437 49	−14.283 8	−23.38 26
	(−7.432 72)[a]	(−14.277 4)[a]	(−23.375 9)[a]
	(−7.419 23)[c]	...	...
f^{2s}_{2s2p}	0.651 27	0.413 15	0.299 63
	(0.767 1)[d]	(0.510 9)[d]	...
α^{2s}_s	171.188	27.383 6	8.994 40
	(164.05)[e]	(24.496 6)[f]	...
I^{2s}_0	3.567 84	12.052 9	25.765 5
	(3.29)[b]	...	...

[a]From Ref. 28.
[b]From Ref. 27.
[c]From Ref. 29.
[d]From Ref. 30.
[e]From Ref. 31.
[f]From Ref. 32.

Sabin.[27] For the valence ($2s$) electron, we obtain orbital energy values of $\epsilon_0^{2s,Li} = -0.201\,16$ a.u., $\epsilon_0^{2s,Be^+} = -0.672\,82$ a.u., and $\epsilon_0^{2s,B^{2+}} = -1.397\,22$ a.u., for the Li, Be^+, and B^{2+} atoms, respectively, with a difference of less than 3% in comparison with the results of Froese-Fischer.[28] However, for the total HF energy, we obtain values with a difference of less than 1% with respect to the results of Froese-Fischer.[28] For the dipole polarizability, we obtain $\alpha_s^{2s,Li} = 171.188$ a.u. and $\alpha_s^{2s,Be^+} = 27.3836$ a.u., in comparison with values of 164.05 a.u. and 24.4966 a.u. reported by Schwerdtfeger and Nagle[31] and Tang *et al.*,[32] respectively.

Thus, our approach using Slater's X-α allows us to account for the ground state properties ϵ_0^{is} and E_{HF} of the Li, Be^+, and B^{2+} atoms, with good agreement with available theoretical results.

In Fig. 1, we show the wavefunctions for the $1s$ and $2s$ orbitals as functions of position r for unconfined Li, Be^+, and B^{2+} atoms. For comparison, we also show the results of Froese-Fischer.[28] We observe excellent agreement for the $1s$ orbital for all ranges. For the $2s$ electron, we also obtain very good agreement for electron distances $r > 1$ a.u. However, we observe that small deviations appear for the inner part of the wavefunction, $r < 1$ a.u., compared with the Froese-Fischer results.

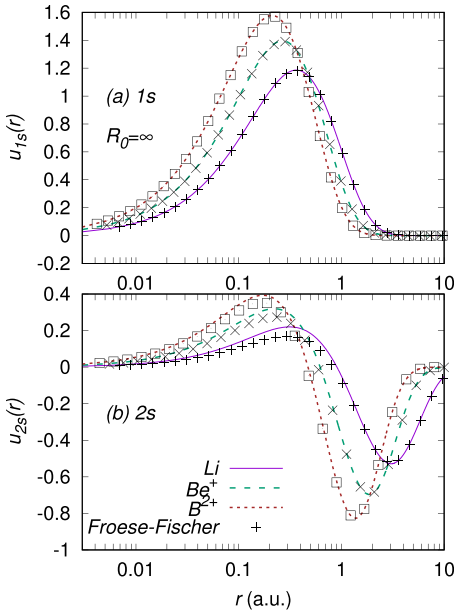

FIG. 1. Wavefunctions for the $1s$ and $2s$ states of Li, Be^+, and B^{2+} atoms as functions of the radial coordinate r for the unconfined atoms. The curves are our results, while the symbols are from Ref. 28.

B. Confined total and orbital HF energies

In Fig. 2, we show the $1s$, $2s$, $2p$, $3s$, and $3p$ energy levels for Li, Be^+, and B^{2+} atoms confined by an impenetrable spherical cavity as a function of the confinement radius R_0. For comparison, we also show the results of Weiss[33] for the free atom energy levels at $R_0 = 30$ a.u. We can see that the energy levels increase, reaching the continuum, as the confinement radius decreases. Furthermore, we observe the appearance of crossing points for the $2s$ and $2p$ energy levels, as well as for the $3s$ and $3p$ levels, which are highlighted by circles for better visualization. Our results confirm the energy level behavior and crossing already reported from other approaches.[34,35] Figure 2(a) shows the $3s$ and $3p$ states of the Li atom. We find that the energy levels reach the continuum for cavities with $R_0 < 10$ a.u. and $R_0 < 12$ a.u., respectively. Here, the $3s$ energy level is deeper than the $3p$ state. As the confinement radius decreases, the $3s$ and $3p$ energy levels increase until a crossing point around $R_0 \sim 6$ a.u. For values of $R_0 < 6$, the $3p$ energy is lower than the $3s$ energy. For the $3s$ and $3p$ states of the Be^+ and B^{2+} atoms, we find a similar trend as for the Li atom. We can see that the crossing points between the $3s$ and $3p$ states of the Li, Be^+, and B^{2+} atoms are in the positive spectrum. For the Be^+ atom, we find that the crossing point occurs at $R_0 \sim 4.6$ a.u.

In Fig. 2(b), we show the $2s$ and $2p$ energy levels, and we can again see an energy increase and the emergence of crossing points as R_0 decreases. We find that the $2p$ energy level of the lithium atom

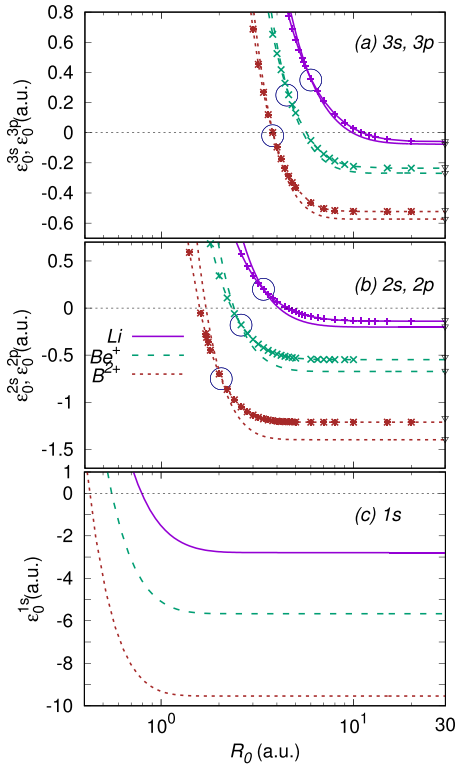

FIG. 2. Orbital energies for the 1*s*, 2*s*, 2*p*, 3*s*, and 3*p* states of Li, Be^+, and B^{2+} atoms confined by a spherical impenetrable cavity as a function of the confinement radius R_0: (a) 3*s* and 3*p* states; (b) 2*s* and 2*p* states; (c) 1*s* ground state. The crossing points between the *ns*–*np* levels are highlighted by circles for better visualization. The curves without symbols are for the *ns* states, while the curves with symbols are for the *np* states. For comparison, the HF results of Weiss[33] for the unconfined atom energy levels are also shown at $R_0 = 30$ a.u (▽).

becomes positive for $R_0 < 4.6$ a.u. and the 2*s* energy level becomes positive for $R_0 < 4.4$ a.u. In this case, the crossing point is present for $R_0 \sim 3.4$ a.u. This cavity size corresponds to a pressure of 85 GPa (see below), which is lower than the 210 GPa reported by Rahm *et al.*[36] The discrepancy is attributed to the different confinement models. The same occurs for the Be^+ atom at a confinement radius of $R_0 \sim 2.5$ a.u. and for B^{2+} at $R_0 \sim 2.1$ a.u. We obtain positive energy values for the 2*s* and 2*p* levels of the Be^+ atom for $R_0 < 2.4$ a.u. and $R_0 < 2.3$ a.u., respectively. For the 2*s* and 2*p* states of the B^{2+} atom, we find positive energies for $R_0 < 1.71$ a.u. and $R_0 < 1.55$ a.u., respectively. Note that since our initial ground state electronic configuration occupies the 2*s* orbital level, for cavities with R_0 lower than the crossing-point radius, one would have photon emission instead of photon absorption for the initial electronic configuration, $1s^2 2s$. We should stress that for R_0 smaller than the critical cavity radius, the lowest-energy state of the Li-like systems becomes *p*-type, and hence the photon emission from the initial *s* to the final *p* states brings the excited electron to its ground state. Once this transition has taken place, as the cavity radius is reduced, the *p*-state evolution lies energetically below the corresponding *s* state, and hence the DOS become positive for excitations.

In Fig. 2(c), we show the 1*s* energy levels as functions of R_0. We find that the effect of the cavity on the 1*s* ground state energy is minimal for $R_0 > 2$ a.u., $R_0 > 1.5$ a.u., and $R_0 > 1$ a.u. for Li, Be^+, and B^{2+} atoms, respectively. For the Li atom, we observe a sudden change in the energy for $R_0 < 2$ a.u. and it reaches a positive value for the 1*s* core state for $R_0 < 0.77$ a.u. A similar situation occurs for the Be^+ atom for $R_0 < 0.555$ a.u. and for B^{2+} for $R_0 < 0.427$ a.u.

The increase in energy is explained as follows. For an impenetrable cavity, the electrons remain localized within the cavity. As the pressure increases, so does the electron kinetic energy (as a consequence of the Heisenberg uncertainty principle), and the total energy can become positive for a critical pressure,[36] as we have just shown, but the system is still bounded.

In Fig. 3, we show the results for the total HF energy for the Li, Be^+, and B^{2+} atoms in the initial $1s^2 2s$ configuration, confined by an impenetrable spherical cavity, as functions of the confinement radius. For comparison, we also show, in the case of Li, the theoretical results of Sañu-Ginarte *et al.*,[29] Le Sech and Banerjee,[37] Sarsa and Le Sech,[38] and Sarsa *et al.*,[13] and we can see that there is excellent agreement. In addition, the HF results for the unconfined atoms obtained by Weiss[33] are shown at $R_0 = 5$ a.u. For the free case, when $R_0 \to \infty$ a.u., we obtain total energies of $E_{HF}^{Li} = -7.437\,49$ a.u., $E_{HF}^{Be^+} = -14.2838$ a.u., and $E_{HF}^{B^{2+}} = -23.3826$ a.u., in good agreement with the values reported by Froese-Fischer[28] and Sañu-Ginarte *et al.*[29] As the confinement radius decreases, the HF energy increases, for all atoms, as previously reported by Connerade *et al.*[39] For the Li, Be^+, and B^{2+} atoms, we observe in Fig. 3 that the effect of the cavity is minimal for $R_0 > 7.3$ a.u., $R_0 > 5.5$ a.u., and $R_0 > 2.5$ a.u., respectively. For the Li atom, for $R_0 < 1.3$ a.u., the HF energy becomes positive. A similar situation occurs for the Be^+ and B^{2+} atoms for $R_0 < 0.94$ a.u. and $R_0 < 0.75$ a.u., respectively.

From Figs. 2 and 3, we conclude that the effect of the confinement cavity is stronger on the valence electrons that on the core electrons.

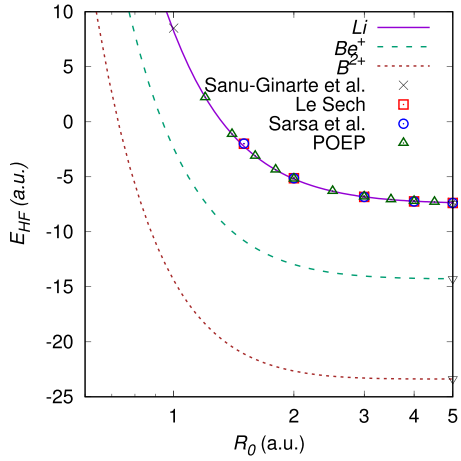

FIG. 3. Total HF energy, Eq. (6), as a function of cavity radius R_0 for Li, Be^+, and B^{2+} atoms. In the case of Li, the symbols show the theoretical results from Sañu-Ginarte *et al.*[29] (×), Le Sech and Banerjee[37] (□), Sarsa and Le Sech[38] (○), and Sarsa *et al.*[13] (△). The HF results for unconfined atoms as reported by Weiss[33] are shown at $R_0 = 5$ a.u (▽).

C. Pressure

The order of magnitude of the pressure that the cavity exerts on the atomic system as R_0 is shrunk is given by the static pressure

$$P = -\frac{\partial E_{\rm HF}}{\partial v} = -\frac{1}{4\pi R_0^2}\frac{\partial E_{\rm HF}}{\partial R_0}, \tag{18}$$

where v is the volume of the spherical cavity. In Fig. 4, we show the results for the pressure as a function of the spherical cavity radius R_0 for Li, Be^+, and B^{2+} atoms. For comparison, we show some characteristic pressures found in nature. We first note that for the same cavity radius, the pressure is lowest for B^{2+}, increases for Be^+, and it is highest for Li. This is a consequence of the ionic character of the system. The lithium atom is more diffuse in its 2*s* orbital, so the same cavity radius induces a higher pressure, while, owing to the high nuclear charge, the boron ion has already compacted its 2*s* electron, so the same cavity radius induces a smaller pressure on the ionic system. The figure also shows the cavity size and pressure for which the $2s \rightarrow 2p$ transition occurs in our approach. For Li, we find it at 85 GPa ($R_0 = 3.4$ a.u.), for Be^+ at 350 GPa ($R_0 = 2.5$ a.u.), and for B^{2+} at 690 GPa ($R_0 = 2.1$ a.u.). These results are within an order of magnitude of those reported by Rahm *et al.*,[36] which were obtained using a different confinement model, thus confirming the suitability of our approach. Rahm *et al.* reported a higher pressure, probably because their model considers penetrable confinement conditions.

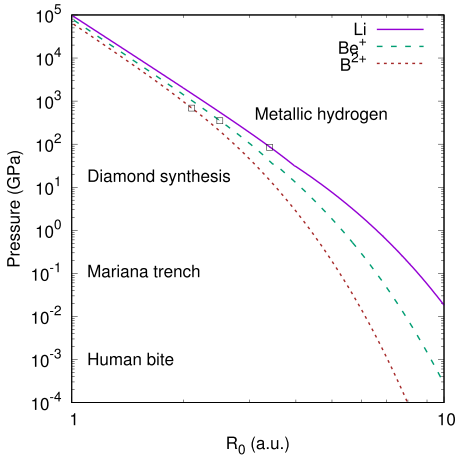

FIG. 4. Static pressure induced by the cavity as a function of cavity size R_0 for Li, Be^+, and B^{2+} atoms confined by an impenetrable spherical cavity. The open square symbols (□) indicate the cavity size and pressure at which the $2s \rightarrow 2p$ transition occurs. Some naturally occurring pressures are also shown.

D. Dipole oscillator strength

In Fig. 5(a), we show the DOS for the electronic transitions $1s \rightarrow 2p$ (core excitations) and $2s \rightarrow 2p$ (valence excitations) for Li, Be^+, and B^{2+} atoms confined by an impenetrable spherical cavity as a function of the confinement radius R_0. In the case of the Li atom, for $R_0 < 15$ a.u., f^{2s}_{2s2p} begins to decrease, showing a change near $R_0 \sim 9$ a.u., where we find a value of $f^{2s}_{2s2p} = 0.588\,95$ a.u. At

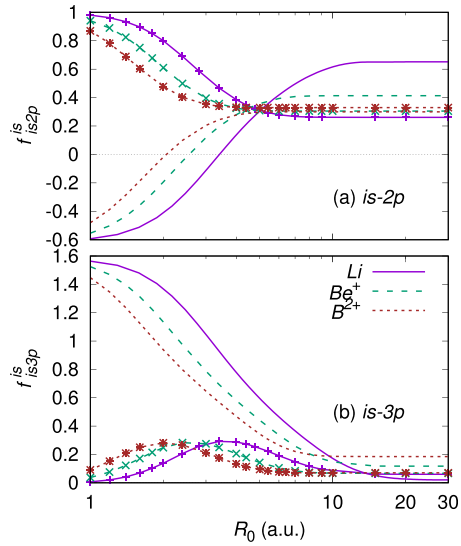

FIG. 5. Dipole oscillator strength for the $is \rightarrow 2p$ and $is \rightarrow 3p$ electronic transitions as a function of the impenetrable spherical cavity size R_0 for Li, Be^+, and B^{2+} atoms for $i = 1$ (core) and $i = 2$ (valence) electrons. The curves without symbols are for the $is \rightarrow 2p$ transition of the valence $i = 2$ electron, while the curves with symbols are for the $i = 1$ core electron.

$R_0 = 6.5$ a.u., we obtain a DOS of 0.460 46 a.u., and at $R_0 = 3.5$ a.u. a value of $f^{2s}_{2s2p} = 0.023\,20$ a.u., near the radius for which the crossing point occurs. For the Be^+ atom, we observe similar behavior. The DOS for the transition decreases rapidly near $R_0 \sim 5$ a.u., with $f^{2s}_{2s2p} = 0.357\,81$ a.u., and then reaches a value of $f^{2s}_{2s2p} = 0.015\,23$ a.u. at $R_0 = 2.6$ a.u., which is near the crossing point. For the B^{2+} atom, we observe the same DOS reduction as R_0 is decreased until the crossing point at $R_0 = 2.1$ a.u. When R_0 is decreased, the DOS for the valence electron excitation, f^{2s}_{2s2p}, is reduced until the 2*s* electron reaches the crossing point between the 2*s* and 2*p* energy levels, so that at that pressure the DOS become zero ($\epsilon_{2s} = \epsilon_{2p}$). Crossing occurs for confinement radii $R_0 \sim 3.4$ a.u., 2.4 a.u., and 2.1 a.u. for Li, Be^+ and B^{2+} atoms, respectively. For confinement radii less than the crossing point, the 2*p* energy levels have lower values than those found for the 2*s* energy level, and there is photon emission induced by the pressure cavity. We should note here that in a sudden approximation perturbation, for a shrinking of the cavity from radius R_0 to $R_0 + \Delta R_0$, the probability of finding the system in the 2*p* state is zero owing to symmetry arguments (orthogonal states). Thus, there is a higher probability for the system to remain in the same *s* symmetry state and then proceed to the 2*p* state by photon emission. Consequently, for a cavity radius lower than the critical crossing point, f^{2s}_{2s2p} becomes negative owing to photon emission, and some other transitions must increase its DOS value to satisfy the TRK sum rule. In Fig. 5(a), we also show the core results for the f^{1s}_{1s2p} transition, and we can see that the DOS increases as R_0 is reduced. f^{1s}_{1s2p} shows an abrupt change near $R_0 \sim 5$ a.u., 3.5 a.u., and 3 a.u. for the Li, Be^+, and B^{2+} atoms, respectively. For lower values of R_0, the DOS transition increases, reaching values near 1 as consequence of confinement, thus becoming a dominant intensity line.

In Fig. 5(b), we show the $1s \rightarrow 3p$ and $2s \rightarrow 3p$ DOS for Li, Be^+, and B^{2+} atoms as functions of the cavity radius. As can be seen, for cavities with radius lower than the critical crossing point, f^{2s}_{2s3p} becomes larger than unity, although the TRK sum rule is satisfied for all cavity radii. Thus, $2s \rightarrow 3p$ becomes the strongest transition, so there is a change in luminosity in the atom as the pressure increases, but in this case due to photon emission induced by the change in pressure, similar to piezoluminescence.[40]

E. Static polarizability

In Fig. 6, we show the static dipole polarizabilities α_s^{2s} and α_s^{1s} for the valence and core states for Li, Be^+, and B^{2+} atoms confined by an impenetrable spherical cavity, as a function of the confinement radius R_0. The crossing points are highlighted by vertical lines. Note that owing to the small contribution of the core electrons, the total atomic polarizability is dominated by the valence contribution for all pressures. For comparison, Fig. 6(a) also shows the unconfined Li and Be^+ results as reported by Schwerdtfeger and Nagle[11] and Tang *et al.*[32] at $R_0 = 30$ a.u., and it can be seen that there is good agreement with our results. For $R_0 \rightarrow \infty$, we obtain the dipole polarizabilities for unconfined lithium-like atoms as $\alpha_s^{2s,\mathrm{Li}} = 171.188$ a.u., $\alpha_s^{2s,\mathrm{Be}^+} = 27.3836$ a.u., and $\alpha_s^{2s,\mathrm{B}^{2+}} = 8.994\,40$ a.u., which exhibit a difference of ~4% with respect to HF results.[11] From Fig. 6, we observe that as the confinement radius decreases, so does the polarizability, until the s–p crossing point is reached. In Fig. 6(a) for the Li atom, for a cavity with radius $R_0 = 4.4$ a.u., the polarizability decreases to 54.2926 a.u., which is about 30% of the free value. As R_0 is reduced, the $2s$ and $2p$ energy levels become positive, and the α_s^{2s} polarizability increases, diverging at $R \sim 3.4$ a.u., which is at the critical crossing point of the $2s$–$2p$ energy levels. For lower values of R_0, α_s^{2s} becomes negative owing to the transition to photon emission. In the case of the Be^+ atom, at $R_0 = 6.5$ a.u., we observe a value of $\alpha_s^{2s} = 26.2083$ a.u., and then the polarizability decreases for lower values of the confinement radius until $R_0 \sim 3.4$ a.u., where a minimum value of $\alpha_s^{2s} = 16.3509$ a.u. is found. Then, for values of $R_0 < 3.4$ a.u., the polarizability increases rapidly, diverging at $R_0 \sim 2.4$ a.u., and it then becomes negative for lower values of R_0. A similar situation occurs for the Be^{2+} atom, but with a minimum value of 6.772 95 a.u. at $R_0 \sim 2.8$ a.u. and a divergence at the crossing point $R_0 \sim 2.1$ a.u. In Fig. 6(b), we show the results for the core contribution α_s^{1s}, where

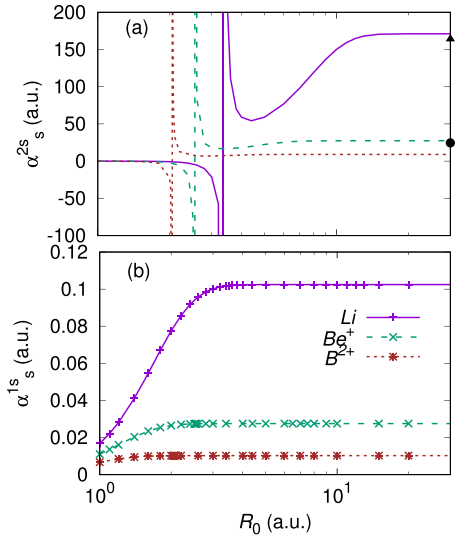

FIG. 6. Static dipole polarizabilities α_s^{2s} (a) and α_s^{1s} (b) as functions of cavity size R_0 for Li, Be^+, and B^{2+} atoms. The solid triangle (▲) and the solid circle (•) at $R_0 = 30$ a.u. are the HF results of Schwerdtfeger and Nagle[11] and Tang *et al.*,[32] respectively.

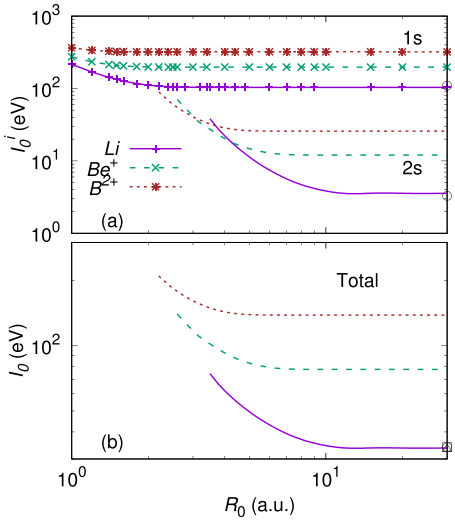

FIG. 7. (a) Mean excitation energies I_0^{1s} (curves with symbols) and I_0^{2s} (curves without symbols) as functions of cavity size R_0 for Li, Be^+, and B^{2+} atoms. For comparison, we also show at $R_0 = 30$ a.u. the values of the free atoms obtained by Oddershede and Sabin[27] (○), Kamakura[41] (△), and Dehmer *et al.*[42] (□). (b) Total mean excitation energy I_0.

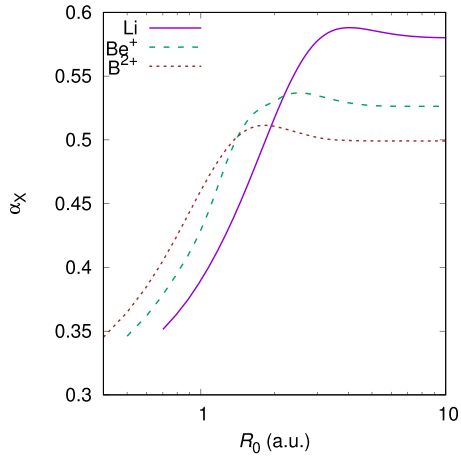

FIG. 8. Slater's X-α parameter α_X as a function of cavity size R_0 for Li, Be^+, and B^{2+} atoms.

TABLE II. Similar to Table I, but for a Li atom confined by an impenetrable spherical cavity for several selected values of the cavity size R_0. The values in parentheses are the theoretical results from Safiu-Ginarte *et al.*[29]

R_0	ϵ_0^{1s}	ϵ_0^{2s}	ϵ_0^{2p}	$E_{\rm HF}$	f_{1s2p}^{1s}	f_{2s2p}^{2s}	f_{2s3p}^{2s}	α_s^{1s}	α_s^{2s}	I_0^{1s}	I_0^{2s}	α_X [Eq. (9)]
0.7	1.320 77	31.446 0	16.934 4	31.131 0	0.990 43	−0.606 48	1.571 51	0.005 35	0.000 16	378.609	...	0.351 35
0.75	0.536 49	26.840 5	14.525 6	25.115 2	0.989 92	−0.605 38	1.571 75	0.006 74	0.000 48	337.266	...	0.357 48
0.79	0.033 49	23.793 8	12.929 2	21.173 3	0.989 19	−0.604 20	1.571 54	0.008 01	0.000 87	309.699	...	0.362 48
0.8	−0.078 06	23.105 9	12.568 3	20.288 0	0.988 97	−0.603 87	1.571 43	0.008 35	0.000 99	303.449	...	0.363 73
1.0	−1.524 94	13.559 0	7.5403 3	8.240 71	0.980 14	−0.593 31	1.564 10	0.016 80	0.006 45	215.303	...	0.389 80
	...	...	...	(8.513 92)	...	...	...	...	...	...	...	...
2.0	−2.749 71	2.002 96	1.295 42	−5.192 26	0.799 73	−0.412 73	1.370 96	0.077 55	0.726 01	111.358	...	0.517 36
	...	...	...	(−5.084 19)	...	...	...	...	...	...	...	...
3.0	−2.791 16	0.415 51	0.343 33	−6.820 14	0.543 18	−0.112 39	1.046 19	0.100 16	21.263 4	103.957	...	0.577 90
4.0	−2.792 33	0.018 79	0.067 24	−7.217 59	0.385 24	0.136 82	0.779 41	0.102 35	58.957 8	103.625	22.106 9	0.588 02
	...	...	...	(−7.185 99)	...	...	...	...	...	...	...	...
5.0	−2.792 36	−0.112 58	−0.040 06	−7.348 98	0.310 79	0.305 19	0.595 47	0.102 45	59.181 9	103.616	11.353 7	0.585 90
	...	...	...	(−7.323 00)	...	...	...	...	...	...	...	...
6.0	−2.792 36	−0.163 46	−0.088 74	−7.399 87	0.279 08	0.418 02	0.465 07	0.102 45	76.600 6	103.616	7.478 42	0.583 19
	...	...	...	(−7.376 79)	...	...	...	...	...	...	...	...
8.0	−2.792 36	−0.194 16	−0.125 16	−7.430 56	0.262 82	0.550 79	0.287 46	0.102 45	118.705	103.616	4.702 04	0.580 69
	...	...	...	(−7.409 85)	...	...	...	...	...	...	...	...
10	−2.792 36	−0.199 96	−0.135 15	−7.436 36	0.261 29	0.614 55	0.172 21	0.102 45	150.076	103.616	3.879 67	0.580 13
	...	...	...	(−7.416 58)	...	...	...	...	...	...	...	...
∞	−2.792 32	−0.201 16	−0.138 81	−7.437 49	0.261 19	0.651 27	0.020 21	0.102 45	171.188	103.613	3.567 84	0.580 02

the effect of the impenetrable cavity starts for $R_0 < 3$ a.u. A decrease in α_s^{1s} is observed for lower values of R_0, where the energy levels become positive. As noted already, the total static dipole polarizability $\alpha_s = 2\alpha^{1s} + \alpha_s^{2s}$ is dominated by the contribution of the valence electron, α_s^{2s}.

F. Mean excitation energy

In Fig. 7, we show the mean excitation energies I_0^{1s}, I_0^{2s}, and I_0, for Li, Be^+, and B^{2+} atoms confined by an impenetrable spherical cavity as functions of the confinement radius R_0. We can see that at $R_0 = 30$ a.u., the results for the free mean excitation energies are in good agreement with previous HF results from Oddershede and Sabin,[27] Kamakura,[41] and Dehmer *et al.*[42] From Fig. 7(a), we can see that as R_0 decreases, I_0^{2s} increases, showing an abrupt change near $R_0 \sim 10$ a.u., 5 a.u., and 4 a.u. for the Li, Be^+, and B^{2+} atoms, respectively, with $I_0^{2s,\rm Li} = 3.879\,67$ eV, $I_0^{2s,\rm Be^+} = 14.739\,33$ eV, and $I_0^{2s,\rm Be^{2+}} = 28.5561$ eV. For the Li valence electron, we observe an increase of ~40% with respect to the free mean excitation energy at $R_0 = 4.4$ a.u. For Be^+, we find an increase of ~11%, and for B^{2+} an increase of ~9% for the same confinement. Figure 7(a) also shows I_0^{1s} for Li, Be^+, and B^{2+} atoms, and we observe an increase in the mean excitation energy as R_0 is reduced. In Fig. 7(b), we show results for the total mean excitation energy I_0. We find $I_0 = 33.708\,90$ a.u., in good agreement with the value of 34.004 13 a.u. obtained by Oddershede and Sabin,[27] Eq. (17), and the value of 34 a.u. reported by Dehmer *et al.*[42] for Li atoms. Note that as a consequence of $2s$–$2p$ energy level crossing, the photon emission produces a negative energy transfer, so the logarithmic contribution is undetermined, as defined by Eqs. (12) and (13). This is observed in the I_0^{2s} contribution and in the total I_0 mean excitation energy for R_0 less than the critical cavity radius at the s–p crossing energy levels. Thus, a different approach may be required to determine it, such as that proposed by Smith *et al.*[43]

G. Slater's X-α contribution

One advantage of Slater's X-α approach is that we can estimate the electron exchange contribution to the energy for a confined quantum system through a single parameter. In Fig. 8, we show the behavior of Slater's X-α parameter α_X as a function of the cavity confinement radius R_0. We find that the largest contribution occurs for the Li atom, followed by the Be^+ ion and then the B^{2+} ion for low-pressure cavities. The contribution increases as R_0 decreases, reaching a maximum, and it then decreases as the cavity becomes small. For the ions, the $2s$ electrons are tighter and the electron exchange parameter is lower for large spherical cavities. However, this behavior is inverted as the cavity increases the pressure. For cavities whose radius is smaller than the critical radius, the α_X parameter is largest for B^{2+}, followed by Be^+, and then Li. So, electron exchange is important as long as the valence electrons remain bounded.

In Tables II and III, for reference purposes, we show the $1s$, $2s$, and $2p$ energy levels, the total HF energy, the first allowed DOS transition $2s \rightarrow 2p$, the dipole polarizability, the mean excitation energy, and Slater's α_X parameter [Eq. (9)] for selected values of the confinement radius R_0 for Li, Be^+, and B^{2+} atoms,

TABLE III. Similar to Table II, but for the Be^+ and B^{2+} atoms.

R_0	ϵ_0^{1s}	ϵ_0^{2s}	ϵ_0^{2p}	E_{HF}	f_{2s2p}^{1s}	f_{2s2p}^{2s}	f_{2s3p}^{2s}	α_s^{1s}	α_s^{2s}	I_0^{1s}	I_0^{2s}	α_X [Eq. (9)]
						Be^+						
0.5	2.137 12	60.173 1	31.471 1	60.325 6	0.990 70	−0.608 33	1.572 96	0.001 41	−0.000 21	737.308	...	0.346 04
0.55	0.123 48	48.159 9	25.269 9	44.587 6	0.990 17	−0.607 04	1.573 59	0.001 94	−0.000 14	628.227	...	0.353 88
0.557	−0.107 08	46.742 9	24.537 9	42.747 0	0.990 03	−0.606 80	1.573 60	0.002 02	−0.000 16	615.258	...	0.354 98
0.57	−0.507 74	44.255 4	23.252 5	39.525 3	0.989 73	−0.606 31	1.573 56	0.002 18	−0.000 21	592.433	...	0.357 06
0.6	−1.312 15	39.150 5	20.612 9	32.954 1	0.988 82	−0.604 97	1.573 17	0.002 58	−0.000 36	545.347	...	0.361 89
0.8	−4.145 59	19.084 9	10.201 9	7.861 46	0.973 72	−0.587 66	1.559 61	0.006 20	−0.003 52	356.727	...	0.395 24
1.0	−5.095 47	10.385 1	5.645 46	−2.410 34	0.940 73	−0.553 61	1.525 12	0.011 02	−0.016 18	274.038	...	0.428 96
2.0	−5.663 14	0.637 48	0.342 34	−12.970 4	0.609 97	−0.194 04	1.134 74	0.026 48	−2.156 21	198.783	...	0.530 27
3.0	−5.667 09	−0.414 12	−0.332 76	−14.025 3	0.395 47	0.118 46	0.787 49	0.027 48	18.111 5	197.523	41.1282	0.534 69
4.0	−5.667 10	−0.614 43	−0.488 48	−14.225 6	0.325 82	0.279 47	0.581 18	0.027 49	18.076 4	197.515	20.3702	0.529 12
5.0	−5.667 09	−0.659 95	−0.531 32	−14.271 2	0.308 63	0.357 81	0.441 37	0.027 49	22.364 1	197.515	14.7393	0.526 99
6.0	−5.667 09	−0.670 23	−0.543 24	−14.281 4	0.305 47	0.393 28	0.336 29	0.027 49	25.356 9	197.515	12.8579	0.526 44
10	−5.667 08	−0.672 89	−0.547 30	−14.284 0	0.304 96	0.413 09	0.147 45	0.027 49	27.374 4	197.514	12.0547	0.526 30
∞	−5.667 11	−0.672 82	−0.547 31	−14.283 8	0.304 97	0.413 15	0.117 10	0.027 49	27.383 6	197.505	12.0529	0.526 32
						B^{2+}						
0.4	2.057 86	91.865 3	47.233 0	90.8137	0.990 79	−0.609 09	1.574 08	0.000 57	0.0	1157.60	...	0.345 26
0.425	0.026 86	79.606 1	40.953 1	74.7372	0.990 50	−0.608 35	1.574 57	0.000 70	0.0	1045.47	...	0.350 04
0.43	−0.328 06	77.419 9	39.832 9	71.8863	0.990 41	−0.608 16	1.574 62	0.000 73	0.0	1025.37	...	0.351 00
0.6	−6.736 88	33.751 6	17.428 1	16.4387	0.978 38	−0.593 42	1.565 24	0.002 07	−0.002 80	614.980	...	0.384 90
0.8	−8.761 85	15.098 4	7.7981 9	−5.712 24	0.938 23	−0.551 23	1.523 06	0.004 37	−0.006 89	435.736	...	0.425 00
1.0	−9.319 56	7.291 26	3.712 27	−14.396 3	0.869 37	−0.480 51	1.447 14	0.006 72	−0.030 34	365.245	...	0.460 22
2.0	−9.541 72	−0.670 23	−0.699 29	−22.656 2	0.477 74	−0.018 72	0.938 65	0.010 21	−22.104 5	321.515	...	0.510 64
3.0	−9.541 95	−1.309 56	−1.135 42	−23.295 7	0.352 20	0.204 47	0.646 29	0.010 24	6.908 57	321.394	40.5256	0.501 88
4.0	−9.541 94	−1.387 56	−1.200 28	−23.373 7	0.331 75	0.277 28	0.469 21	0.010 24	8.205 13	321.394	28.5561	0.499 53
5.0	−9.541 93	−1.396 37	−1.209 33	−23.382 5	0.329 76	0.295 81	0.343 88	0.010 24	8.831 21	321.393	26.1855	0.499 23
6.0	−9.541 92	−1.397 17	−1.210 37	−23.383 3	0.329 64	0.299 16	0.264 51	0.010 24	8.970 87	321.392	25.8135	0.499 20
10	−9.541 89	−1.397 23	−1.210 49	−23.383 3	0.329 63	0.299 66	0.186 63	0.010 24	8.993 81	321.390	25.7654	0.499 20
∞	−9.541 58	−1.397 22	−1.210 49	−23.382 6	0.329 65	0.299 63	0.184 99	0.010 24	8.994 40	321.368	25.7655	0.499 22

IV. CONCLUSIONS

We have studied lithium-like atoms confined by an impenetrable spherical cavity of radius R_0. We find good to excellent agreement when comparing orbital and total energies, as well as when determining dipole transitions, static polarizability, and mean excitation energies for the unconfined systems. For the lithium atom, we find excellent agreement for confined ground state energies in comparison with available theoretical results.

We confirm that, as a consequence of the confinement, the system orbital and total energies increase as the pressure increases owing to a reduction in cavity size. However, the first allowed dipole transition, $2s \rightarrow 2p$, decreases, while $2s \rightarrow 3p$ increases. Consequently, as the pressure increases, the intensity of light emitted by the atom in the cavity is shifted. However, there is a crossing point (critical pressure) at which the $2s$ and $2p$ energy levels are inverted; consequently, the DOS for that transition becomes zero at that critical pressure. For higher pressures, the DOS become negative owing to photon emission. In addition, the $2s \rightarrow 3p$ DOS reach values larger than unity for high pressures, and the $2s \rightarrow 2p$ DOS becomes negative. Thus, we can confirm that the static dipole polarizability is reduced as the pressure increases, as the electrons become highly localized within the cavity and less prone to be polarized, and diverges at the point of transition from photon absorption to photon emission. We also find that the mean excitation energy, which measures the ability of the atom to absorb energy due to excitations, increases as the pressure is increased, with implications for material damage under extreme conditions. As a result of the existence of the crossing point, the valence and total mean excitation energy become undetermined owing to a logarithmic indeterminacy, and thus a different approach may be required.

Our work shows the reliability of Slater's X-α approach in the context of HF theory to study confined N-electron quantum systems. This approach has the advantage that it can be extended to larger systems to provide excitation spectra in different confinement environments, thus shedding light on the behavior of N-body quantum systems under extreme conditions.

ACKNOWLEDGMENTS

C.M.-F. thanks CONACyT for a postdoctoral fellowship through Project No. FC-2016/2412, as well as for the hospitality of the chemistry department at UAM-I. R.C.-T. would like to thank DGAPA-UNAM PAPIIT-IN-106-617, LANCAD-UNAM-DGTIC-228, and DGAPA-PASPA for support, as well as the University of Heidelberg for its hospitality.

REFERENCES

[1]A. Michels, J. De Boer, and A. Bijl, "Remarks concerning molecural interaction and their influence on the polarisability," Physica **4**(10), 981–994 (1937).
[2]*Advances in Quantum Chemistry*, edited by S. A. Cruz, J. Sabin, and E. Brandas (Elsevier, Amsterdam, 2009), Vol. 57.
[3]*Advances in Quantum Chemistry*, edited by S. A. Cruz, J. Sabin, and E. Brandas (Elsevier, Amsterdam, 2009), Vol. 58.
[4]*Electronic Structure of Quantum Confined Atoms and Molecules*, edited by K. D. Sen (Springer International Publishing, Switzerland, 2014).
[5]W. Jaskólski, "Confined many-electron systems," Phys. Rep. **271**(1), 1–66 (1996).
[6]E. Ley-Koo, "Recent progress in confined atoms and molecules: Superintegrability and symmetry breakings," Rev. Mex. Fis. **64**, 326–363 (2018).
[7]G. McGinn, "Atomic and molecular calculations with the pseudopotential method. VII One-valence-electron photoionization cross sections," J. Chem. Phys. **53**(9), 3635–3640 (1970).
[8]J. N. Bardsley, "Pseudopotential calculations of alkali interactions," Chem. Phys. Lett. **7**(5), 517–520 (1970).
[9]P. G. Burke and W. D. Robb, "The r-matrix theory of atomic processes," Adv. At. Mol. Phys. **11**, 143–214 (1976).
[10]G. Peach, H. E. Saraph, and M. J. Seaton, "Atomic data for opacity calculations. IX. The lithium isoelectronic sequence," J. Phys. B: At., Mol. Opt. Phys. **21**(22), 3669 (1988).
[11]P. Schwerdtfeger, "The pseudopotential approximation in electronic structure theory," ChemPhysChem **12**(17), 3143–3155 (2011).
[12]C. Y. Lin and Y. K. Ho, "Photoionization of atoms encapsulated by cages using the power-exponential potential," J. Phys. B: At., Mol. Opt. Phys. **45**(14), 145001 (2012).
[13]A. Sarsa, E. Buendía, and F. J. Gálvez, "Study of confined many electron atoms by means of the POEP method," J. Phys. B: At., Mol. Opt. Phys. **47**(18), 185002 (2014).
[14]J. W. Cooper, "Photoionization from outer atomic subshells. A model study," Phys. Rev. **128**, 681–693 (1962).
[15]E. V. Ludeña, "SCF Hartree-Fock calculations of ground state wavefunctions of compressed atoms," J. Chem. Phys. **69**(4), 1770–1775 (1978).
[16]J. C. Slater, "A simplification of the Hartree-Fock method," Phys. Rev. **81**, 385–390 (1951).
[17]A. Zangwill, "A half century of density functional theory," Phys. Today **68**(7), 34–39 (2015).
[18]A. Szabo and N. S. Ostlund, *Modern Quantum Chemistry: Introduction to Advanced Electronic Structure Theory*, 1st ed. (Dover Publications Inc., New York, 1996).
[19]M. S. Pindzola, "Excitation and charge transfer in proton-lithium collisions at 5–15 kev," Phys. Rev. A **60**, 3764–3768 (1999).
[20]M. Miyasita, K. Higuchi, and M. Higuchi, "An alternative scheme for calculating the unrestricted Hartree–Fock equation: Application to the boron and neon atoms," Physica B **407**(14), 2758–2762 (2012).
[21]R. Cabrera-Trujillo and S. A. Cruz, "Confinement approach to pressure effects on the dipole and the generalized oscillator strength of atomic hydrogen," Phys. Rev. A **87**, 012502 (2013).
[22]S. Koonin and D. C. Meredith, *Computational Physics: Fortran Version* (Westview Press, 1998).
[23]M. Inokuti, "Inelastic collisions of fast charged particles with atoms and molecules—The Bethe theory revisited," Rev. Mod. Phys. **43**, 297–347 (1971).
[24]H. Friedrich, *Theoretical Atomic Physics*, 3rd ed. (Springer-Verlag, Berlin Heidelberg, 2006).
[25]H. A. Bethe and R. Jackiw, *Intermediate Quantum Mechanics*, 3rd ed. (Westview Press, Boulder, Colo, EE.UU., 1997).
[26]H. Bethe, "Zur theorie des durchgangs schneller korpuskularstrahlen durch materie," Ann. Phys. **397**(3), 325–400 (1930).
[27]J. Oddershede and J. R. Sabin, "Orbital and whole-atom proton stopping power and shell corrections for atoms with $z < 36$," At. Data Nucl. Data Tables **31**(2), 275–297 (1984).
[28]C. Froese-Fischer, "A general multi-configuration Hartree-Fock program," Comput. Phys. Commun. **14**(1-2), 145–153 (1978).
[29]A. D. Sañu-Ginarte, E. M. Guillén-Romero, L. Ferrer-Galindo, L. A. Ferrer-Moreno, R. Betancourt-Riera, and R. Riera, "New approach to obtain the analytical expression of the energy functional in free or confined atoms," Results Phys. **13**, 102261 (2019).
[30]A. W. Weiss, "The calculation of atomic oscillator strengths: The lithium atom revisited," Can. J. Chem. **70**(2), 456–463 (1992).
[31]P. Schwerdtfeger and J. K. Nagle, "2018 Table of static dipole polarizabilities of the neutral elements in the periodic table," Mol. Phys. **117**(9-12), 1200–1225 (2019).
[32]L.-Y. Tang, Z.-C. Yan, T.-Y. Shi, and J. Mitroy, "Dynamic dipole polarizabilities of the Li atom and the Be^+ ion," Phys. Rev. A **81**, 042521 (2010).
[33]A. W. Weiss, "Wave functions and oscillator strengths for the lithium isoelectronic sequence," Astrophys. J. **138**, 1262 (1963).
[34]J. P. Connerade, V. K. Dolmatov, and P. A. Lakshmi, "The filling of shells in compressed atoms," J. Phys. B: At., Mol. Opt. Phys. **33**(2), 251 (2000).
[35]J. P. Connerade and R. Semaoune, "Atomic compressibility and reversible insertion of atoms into solids," J. Phys. B: At., Mol. Opt. Phys. **33**(17), 3467–3484 (2000).
[36]M. Rahm, R. Cammi, N. W. Ashcroft, and R. Hoffmann, "Squeezing all elements in the periodic table: Electron configuration and electronegativity of the atoms under compression," J. Am. Chem. Soc. **141**(26), 10253–10271 (2019).
[37]C. Le Sech and A. Banerjee, "A variational approach to the dirichlet boundary condition: Application to confined H^-, He and Li," J. Phys. B: At., Mol. Opt. Phys. **44**(10), 105003 (2011).
[38]A. Sarsa and C. Le Sech, "Variational Monte Carlo method with Dirichlet boundary conditions: Application to the study of confined systems by impenetrable surfaces with different symmetries," J. Chem. Theory Comput. **7**(9), 2786–2794 (2011).
[39]J. P. Connerade, P. Kengkan, P. Anantha Lakshmi, and R. Semaoune, "Scaling laws for atomic compressibility," J. Phys. B: At., Mol. Opt. Phys. **33**(22), L847–L854 (2000).
[40]N. A. Atari, "Piezoluminescence phenomenon," Phys. Lett. A **90**(1), 93–96 (1982).
[41]S. Kamakura, N. Sakamoto, H. Ogawa, H. Tsuchida, and M. Inokuti, "Mean excitation energies for the stopping power of atoms and molecules evaluated from oscillator-strength spectra," J. Appl. Phys. **100**(6), 064905 (2006).
[42]J. L. Dehmer, M. Inokuti, and R. P. Saxon, "Systematics of moments of dipole oscillator-strength distributions for atoms of the first and second row," Phys. Rev. A **12**, 102–121 (1975).
[43]D. Y. Smith, M. Inokuti, W. Karstens, and E. Shiles, "Mean excitation energy for the stopping power of light elements," Nucl. Instrum. Methods Phys. Res., Sect. B **250**(1), 1–5 (2006), Part of special issue on Radiation Effects in Insulators.